Modeling and Estimation of FPN Components in CMOS Image Sensors

Abbas El Gamal[a], Boyd Fowler[a], Hao Min[b], Xinqiao Liu[a]

[a]Information Systems Laboratory, Stanford University
Stanford, CA 94305 USA

[b]Fudan University, Shanghai China

ABSTRACT

Fixed pattern noise (FPN) for a CCD sensor is modeled as a sample of a spatial white noise process. This model is, however, not adequate for characterizing FPN in CMOS sensors, since the readout circuitry of CMOS sensors and CCDs are very different. The paper presents a model for CMOS FPN as the sum of two components: a column and a pixel component. Each component is modeled by a first order isotropic autoregressive random process, and each component is assumed to be uncorrelated with the other. The parameters of the processes characterize each component of the FPN and the correlations between neighboring pixels and neighboring columns for a batch of sensors. We show how to estimate the model parameters from a set of measurements, and report estimates for 64×64 passive pixel sensor (PPS) and active pixel sensor (APS) test structures implemented in a 0.35 micron CMOS process. High spatial correlations between pixel components were measured for the PPS structures, and between the column components in both PPS and APS. The APS pixel components were uncorrelated.

Keywords: CMOS image sensor, fixed pattern noise, nonuniformity, image sensor characterization

1. INTRODUCTION

Fixed pattern noise (FPN) is the variation in output pixel values, under uniform illumination, due to device and interconnect mismatches across an image sensor. In a CCD image sensor FPN is modeled as a sample from a spatial white noise process*. This is justified by the fact that in a typical CCD sensor all pixels share the same output amplifier. As a result FPN is mainly due to variations in photodetector area and dark current, which are spatially uncorrelated. To estimate FPN for a CCD sensor output values are read out multiple times for each pixel at the same constant monochromatic illumination and an average pixel value is computed. The averaging reduces random noise and the remaining pixel output variations are the FPN. A single summary statistic of the FPN, usually the standard deviation of the averaged pixel values, is adequate to characterize the FPN since the output values are uncorrelated.[1]

This white noise model is not adequate for characterizing FPN in CMOS sensors because the readout circuitry for CMOS sensors and CCDs are very different. As depicted in Figures 1 and 2 the readout signal paths for both CMOS passive and active pixel sensors (PPS and APS) include several amplifiers some of which are shared by pixels and some are not. These amplifiers introduce additional FPN, which is not present in CCDs. In particular the FPN due to variations in column amplifier offsets and gains causes "striped" noise, which has a very different spatial structure than the white noise observed in CCDs. Even though the offset part of this column FPN is significantly reduced using correlated double sampling (CDS), the gain part is not. Therefore, to adequately characterize CMOS FPN, we must estimate separately factors associated with pixel to pixel variation, and column to column variation.

In this paper we introduce a statistical model for FPN in CMOS sensors. We represent FPN as the sum of two components: a column and a pixel component. Each component is modeled by a first order isotropic autoregressive process, and the processes are assumed to be uncorrelated. The process parameters characterize the standard deviation of each FPN component and the spatial correlations between pixels and columns for a batch of sensors.

Other author information: Email: abbas@isl.stanford.edu, fowler@isl.stanford.edu, minhao@isl.stanford.edu, chiao@isl.stanford.edu; Telephone: 650-725-9696; Fax: 650-723-8473

*A spatial white noise random process is a set of zero mean uncorrelated random variables with the same standard deviation. If the random variables are gaussian, the noise is completely specified by the standard deviation of the random variables.

This model can be used to measure the quality of a batch of sensors by comparing the model parameters to their nominal values, or to simulate FPN by drawing samples from the processes.

In Section 2 we describe our FPN model and show how to estimate its parameters. In section 3 we report measurements and results using our 64×64 PPS and APS test structures[2] implemented in a 0.35 micron CMOS process. The results show high spatial correlations between pixel FPN components for the PPS structures, but virtually no correlation between the APS pixel FPN components. Correlations were observed between the column FPN components in both PPS and APS. These results appear to be consistent with the nature of the spatial variations of the different FPN sources, but as discussed in Section 4 more work remains to be done to validate our proposed FPN model.

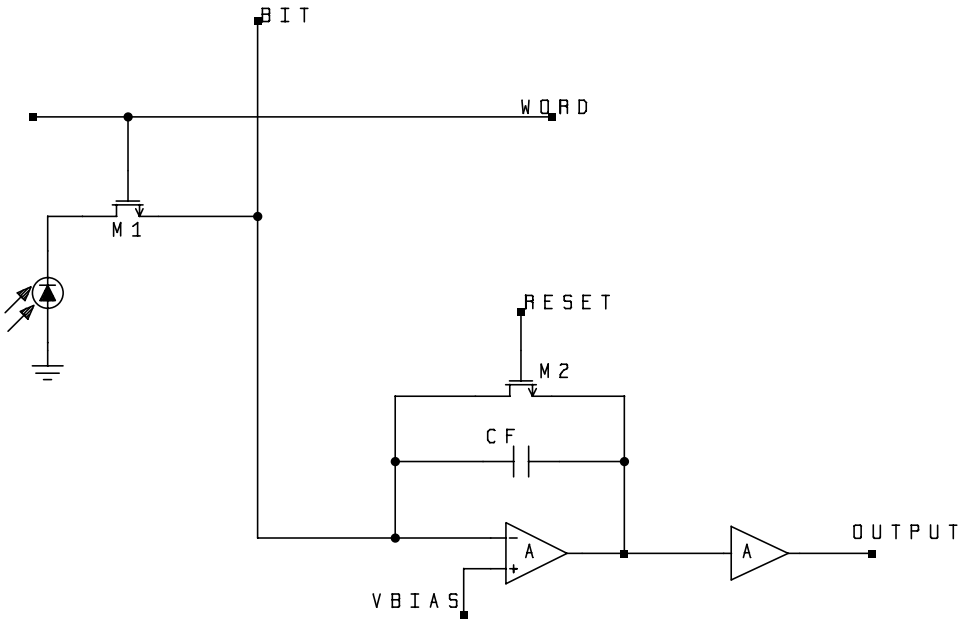

Figure 1. PPS signal path. Pixel FPN is caused by photodiode leakage, variations in photodiode area, channel charge injection from M1, and capacitive coupling from the overlap capacitance of M1. Column FPN is caused by offset in the integrating amplifier(*), size variations in the integrating capacitor CF, channel charge injection from M2(*), capacitive coupling from the overlap capacitance of M2(*), and threshold variations in M2(*). FPN components that are reduced by CDS are marked with (*).

2. MODELING AND ESTIMATION

Assuming constant monochromatic illumination we model FPN as a two dimensional random process (random field) $F_{i,j}$ where the $F_{i,j}$s are zero mean random variables representing the deviation of the output pixel values from the pixel value with no added random noise, and i and j are the row and column index respectively. To capture the structure of FPN in a CMOS sensor we express $F_{i,j}$ as the sum of a column FPN component Y_j and a pixel FPN component $X_{i,j}$. Thus,

$$F_{i,j} = Y_j + X_{i,j}, \tag{1}$$

where the Y_js and the $X_{i,j}$s are zero mean random variables.

The goal of this work is to devise an FPN model to be used for measuring the quality for a batch of sensors or to simulate FPN, e.g. in a digital camera simulator. We would like the model to be simple, but accurate enough,

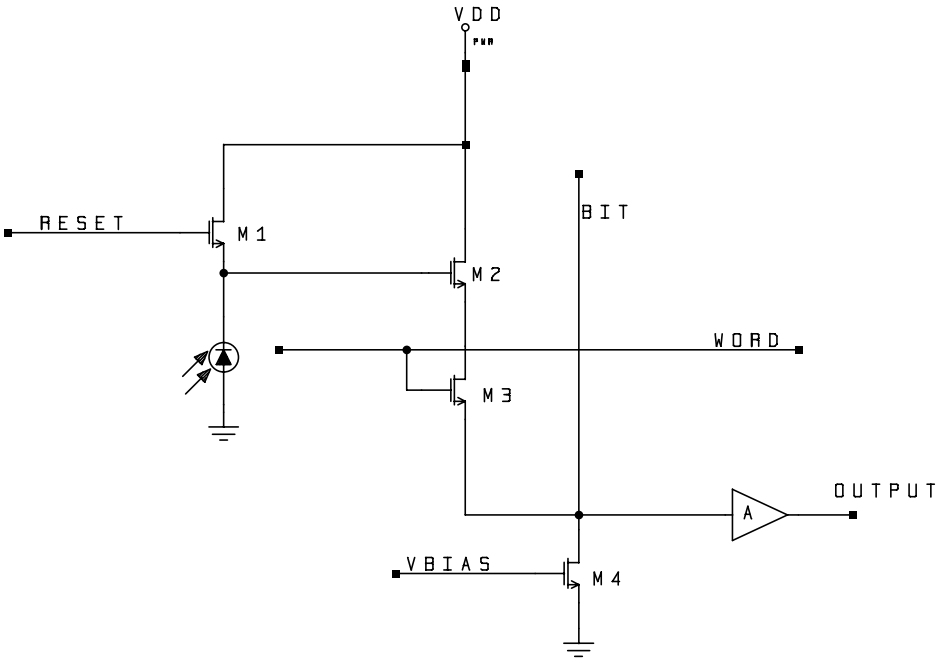

Figure 2. APS signal path. Pixel FPN is caused by photodiode leakage, variations in photodiode size, variations in photodiode capacitance, channel charge injection from M1(*), capacitive coupling from the overlap capacitance of M1(*), threshold variations in M1(*), and threshold variations in M2(*). Column FPN is caused by variations in bias current (M4)(*), offset in the column amplifier, and gain variations in the column amplifier. FPN components that are reduced by CDS are marked with (*).

with as few parameters as possible so that good estimates can be developed. We therefore make several simplifying assumptions.

The first assumption we make is that the random processes Y_j and $X_{i,j}$ are uncorrelated, i.e. that $E[Y_j X_{i,k}] = 0$ for all i, j, and k. This assumption is reasonable since the column and pixel FPN are caused by different device parameter variations (see Figures 1 and 2). We further assume that the column (and pixel) FPN processes are isotropic. Thus the autocorrelation functions for the processes Y_j and $X_{i,j}$s are space invariant. Since FPN depends on device variations which tend to increase with the distance between the devices on the chip, we assume that the correlation between pixels (or columns) decreases as a function of the distance between them.

We propose to use autoregressive processes to model FPN because their parameters can be easily and efficiently estimated from data. In this paper we only consider the simplest such model, namely first order isotropic autoregressive processes. The work presented can be extended to higher order models. However, the results suggest that additional model complexity may not be warranted.

Our model assumes that the column FPN process Y_j is a first order isotropic autoregressive process of the form:

$$Y_j = a(Y_{j-1} + Y_{j+1}) + U_j, \tag{2}$$

where the U_js are zero mean, uncorrelated random variables with the same variance σ_U^2, and $0 \leq a \leq \frac{1}{2}$ is a parameter that characterizes the dependency of Y_j on its two neighbors . The autocorrelation function $R_Y(n) = E[Y_j Y_{j+n}]$ of the process Y_j must satisfy the recurrence equations:

$$R_Y(0) = {\sigma^2}_Y = 2aR_Y(1) + R_{YU}(0), \tag{3}$$

$$R_{YU}(0) = 2aR_{YU}(1) + \sigma_U^2, \tag{4}$$

$$R_Y(n) = a(R_Y(n-1) + R_Y(n+1)) + R_{YU}(n), \text{ and} \tag{5}$$

$$R_{YU}(n) = a(R_{YU}(n-1) + R_{YU}(n+1)) \tag{6}$$

for $|n| \geq 1$.

To estimate the model parameters σ_U^2 and a, we first estimate ${\sigma^2}_Y$ and $R_Y(1)$ (using the estimators in equations 15, 17, and 19). We express

$$R_Y(1) = \rho_Y {\sigma^2}_Y, \tag{7}$$

where $0 \leq \rho_Y \leq 1$. Thus ρ_Y can be directly estimated from the estimates of ${\sigma^2}_Y$ and $R_Y(1)$. It can be verified using the recurrence equations 3, 4, 5 and 6 that

$$a = \frac{\rho_Y}{2}, \text{ and} \tag{8}$$

$$\sigma_U^2 = \sigma_Y^2 (1 - \rho_Y)^{\frac{3}{2}}. \tag{9}$$

Thus once σ_Y^2 and ρ_Y are estimated equations 8 and 9 can be used to estimate a and σ_U^2.

Our model assumes that the pixel FPN process $X_{i,j}$ is a two dimensional first order isotropic autoregressive process of the form:

$$X_{i,j} = b(X_{i-1,j} + X_{i+1,j} + X_{i,j-1} + X_{i,j+1}) + V_{i,j}, \tag{10}$$

where the $V_{i,j}$s are zero mean uncorrelated random variables with the same variance σ_V^2, and $0 \leq b \leq \frac{1}{4}$ is a parameter that characterizes the dependency of $X_{i,j}$ on its four neighbors. The autocorrelation function $R_X(m,n) = E[X_{i,j}X_{i+m,j+n}] = R_X(n,m)$ and the crosscorrelation function $R_{XV}(m,n) = E[X_{i,j}V_{i+m,j+n}] = R_{XV}(n,m)$ satisfy the recurrence equations

$$R_X(0,0) = {\sigma^2}_X = 4bR_X(0,1) + R_{XV}(0,0), \tag{11}$$

$$R_{XV}(0,0) = 4bR_{XV}(0,1) + {\sigma^2}_V, \tag{12}$$

$$R_X(n,m) = b(R_X(n-1,m) + R_X(n+1,m) + R_X(n,m-1) + R_X(n,m+1)) + R_{XV}(n,m), \text{and} \tag{13}$$

$$R_{XV}(n,m) = b(R_{XV}(n-1,m) + R_{XV}(n+1,m) + R_{XV}(n,m-1) + R_{XV}(n,m+1)) \tag{14}$$

for $|n|$, or $|m| \geq 1$. To estimate the model parameters σ_V^2 and b we first estimate σ_X^2 and $R_X(1,0) = R_X(0,1)$ using the estimators given in equations 15, 16, 18, and 20). Although it may be possible to solve the above recurrence equations analytically we use the simple numerical method described in APPENDIX A. An advantage of this method is that it can be readily used for more complex models.

Now to estimate the parameters of the model we measure pixel output values for a subsensor array of $N \times M$ pixels under constant illumination. We repeat this measurement P times and average the values for each pixel to reduce the effect of random noise on the output values. We then compute the sample average output pixel value and subtract it off the averaged values to obtain estimates of the $F_{i,j}$s. To simplify our analysis we assume that these estimates are perfect, i.e. that we know the values of the $F_{i,j}$s.

To estimate Y_j, $X_{i,j}$, σ_Y^2, σ_X^2, $R_Y(1)$, and $R_X(0,1)$ we use the following estimators:

$$\overline{Y_j} = \frac{1}{N} \sum_{i=1}^{N} F_{i,j}, \tag{15}$$

$$\overline{X_{i,j}} = F_{i,j} - \overline{Y_j}, \tag{16}$$

$$\overline{\sigma_Y^2} = \frac{1}{M-1} \sum_{j=1}^{M} \overline{Y_j}^2, \tag{17}$$

$$\overline{\sigma_X^2} = \frac{1}{M(N-1)} \sum_{i=1}^{N} \sum_{j=1}^{M} \overline{X_{i,j}}^2, \tag{18}$$

$$\overline{R_Y(1)} = \frac{1}{M-1} \sum_{i=1}^{M-1} \overline{Y_j}\ \overline{Y_{j+1}}, \text{ and} \tag{19}$$

$$\overline{R_X(0,1)} = \frac{1}{2N(M-1)} \sum_{i=1}^{N} \sum_{j=1}^{M-1} \overline{X_{i,j} X_{i,j+1}} + \frac{1}{2M(N-1)} \sum_{i=1}^{N-1} \sum_{j=1}^{M} \overline{X_{i,j} X_{i+1,j}}. \tag{20}$$

3. RESULTS

In this section we present the measured FPN results from our 64×64 pixel PPS and APS test structures[2] fabricated in a 0.35μm digital CMOS process. A summary of the main test structure characteristics are provided in Table 1.

	PPS	APS
Technology	0.35 μm, 4-layer metal 1-layer poly, nwell CMOS	0.35 μm, 4-layer metal 1-layer poly, nwell CMOS
Number of Pixels	64×64	64×64
Pixel Area	14μm×14μm	14μm×14μm
Transistors per pixel	1	3
Fill Factor	37%	29%
Photodetector	nwell/psub diode	nwell/psub diode
Pixel Interconnect	Metal1 and Poly	Metal1 and Poly

Table 1. Test Structure Characteristics in 0.35μm CMOS Technology

The setup used to measure FPN is described by Fowler et al..[3] It consists of a DC light source, a monochromator, an integrating sphere, and a calibrated photodiode. The measurements were performed under no illumination (dark) and at typical illumination using a monochromatic source, of wavelength $\lambda = 600$nm. At the beginning of each array measurement, all pixels are reset. The data is then read out after an integration time of 50ms. The data from each pixel consists of a signal sample and a reset sample. Each of the signal and the reset samples are amplified using a very low noise amplifier and then digitized using a 16 bit ADC. The amplifier is used to match the output swing of the sensor to the input range of the ADC. The array measurement is repeated $P = 1024$ times for each chip. These measurements are performed for eight PPS and eight APS chips with and without illumination. The chosen level of illumination results in an output signal that is 70% of the maximum output signal swing.

The FPN results for the PPS and APS test structures with and without illumination are presented in Tables 2 and 3, respectively. The tables present the estimated standard deviation and autocorrelation values averaged over the eight chips and the derived process parameters based on the averaged estimates. All values are reported in equivalent input electrons. To find the input electron numbers we normalized the measured output voltage values using the estimated gain numbers obtained from our QE measurements.[3] These results translate into estimated dark FPN of 1.7% and 0.15% of full well capacity for PPS and APS respectively.

The results clearly show that CDS reduces FPN for both PPS and APS. It also shows that CDS is far less effective with illumination than without illumination. After CDS the PPS FPN is higher than that of the APS. The fact that PPS column FPN is larger than that for APS is easily explained by the additional column charge integrating amplifier used in PPS. The higher PPS pixel FPN may be attributed to the charge injection from the overlap capacitance transistor which is not canceled by CDS. It may also be due to the bias in the estimators.

The FPN correlation between pixels is high for PPS and low for APS. This suggests that variations in column amplifier offset, charge injection, and capacitive coupling, which dominate pixel FPN in PPS are highly correlated, while pixel area and dark current, which dominate pixel FPN in APS, vary rapidly from pixel to pixel.

To compare our model with the measured data we generated 64×64 sample FPN images using the model parameters in Tables 2 and 3. The measured and simulated FPN images for PPS and APS with and without CDS are shown in Figures 3 and 4, respectively. To display the FPN images we scaled each non-CDS image so that the maximum pixel value range is 8-bits. Each CDS image was then scaled using the same scale factor as its non-CDS counterpart. Note that the APS images use a scale factor that is eight times smaller than that for the PPS images. These images demonstrate that our model closely predicts FPN for PPS and APS.

	PPS with CDS	PPS without CDS	APS with CDS	APS without CDS
Estimated Statistics:				
$\overline{\sigma_Y^2}$ (electrons^2)	53519470	647555000	145550	343326
$\overline{\sigma_{\sigma_Y^2}}$ (electrons^2)	458044	17932700	7851	60456
$\overline{R_Y(1)}$ (electrons^2)	12255300	61853600	20862	100255
$\overline{\sigma_{R_Y(1)}}$ (electrons^2)	1728000	1299050	4085	12704
$\overline{\sigma_X^2}$ (electrons^2)	4584010	4582680	597282	5619600
$\overline{\sigma_{\sigma_X^2}}$ (electrons^2)	128423	144732	7133	114361
$\overline{R_X(0,1)}$ (electrons^2)	2217790	2211580	46763	306332
$\overline{\sigma_{R_X(0,1)}}$ (electrons^2)	83427	89529	3478	17288
Estimated Paramters:				
$\overline{a}$	0.11	0.05	0.09	0.15
$\overline{\sigma_U^2}$ (electrons^2)	36232900	557027000	87332	186633
$\overline{b}$	0.19	0.19	0.04	0.03
$\overline{\sigma_V^2}$ (electrons^2)	2321600	2320900	585761	5558750

Table 2. Estimated statistics and parameters under uniform illumination (≈70% full well). The statistics are averaged over all 8 chips. Note that $\overline{\sigma_{\sigma_Y^2}}$, $\overline{\sigma_{R_Y(1)}}$, $\overline{\sigma_{\sigma_X^2}}$, and $\overline{\sigma_{R_X(0,1)}}$ are the estimated standard deviations of the estimators.

	PPS with CDS	PPS without CDS	APS with CDS	APS without CDS
Estimated Statistics:				
$\overline{\sigma_Y^2}$ (electrons^2)	6569330	317322000	80900	451611
$\overline{\sigma_{\sigma_Y^2}}$ (electrons^2)	45364	16521500	32747	68787
$\overline{R_Y(1)}$ (electrons^2)	596727	14011000	7421	159550
$\overline{\sigma_{R_Y(1)}}$ (electrons^2)	119797	3122460	5374	17057
$\overline{\sigma_X^2}$ (electrons^2)	151812	146100	4155	7144450
$\overline{\sigma_{\sigma_X^2}}$ (electrons^2)	10883	14329	1660	105369
$\overline{R_X(0,1)}$ (electrons^2)	122902	120067	36	442880
$\overline{\sigma_{R_X(0,1)}}$ (electrons^2)	6891	9524	56	41255
Estimated Paramters:				
$\overline{a}$	0.05	0.02	0.05	0.18
$\overline{\sigma_U^2}$ (electrons^2)	5694860	296539000	70029	234866
$\overline{b}$	0.24	0.24	0.01	0.03
$\overline{\sigma_V^2}$ (electrons^2)	19949	19199	214	7067090

Table 3. Estimated statistics and parameters under dark conditions. The statistics are averaged over all 8 chips. Note that $\overline{\sigma_{\sigma_Y^2}}$, $\overline{\sigma_{R_Y(1)}}$, $\overline{\sigma_{\sigma_X^2}}$, and $\overline{\sigma_{R_X(0,1)}}$ are the estimated standard deviations of the estimators.

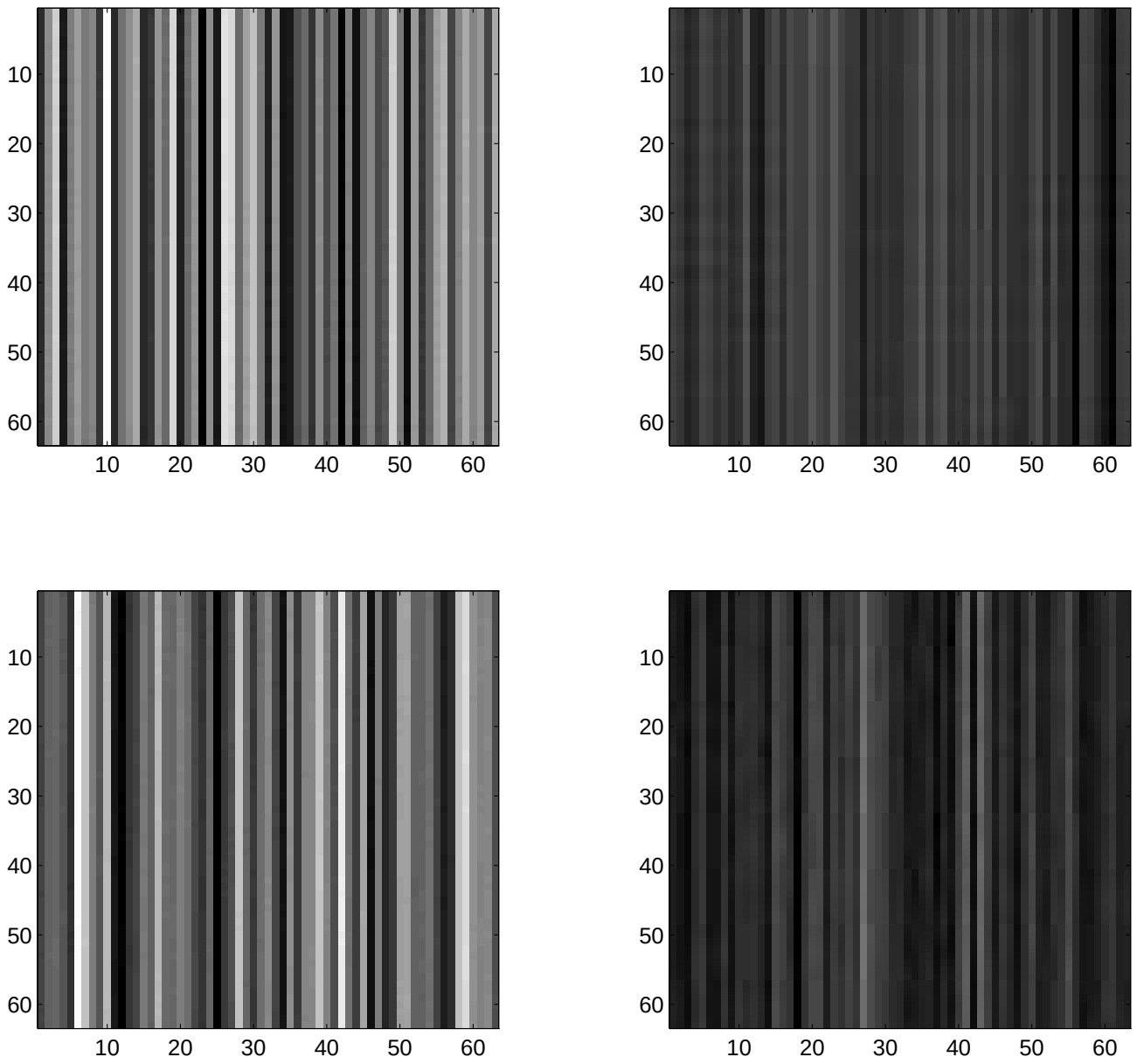

Figure 3. Top left – measured PPS FPN without CDS, top right – measured PPS FPN with CDS, bottom left – simulated PPS FPN without CDS, and bottom right – simulated PPS FPN with CDS.

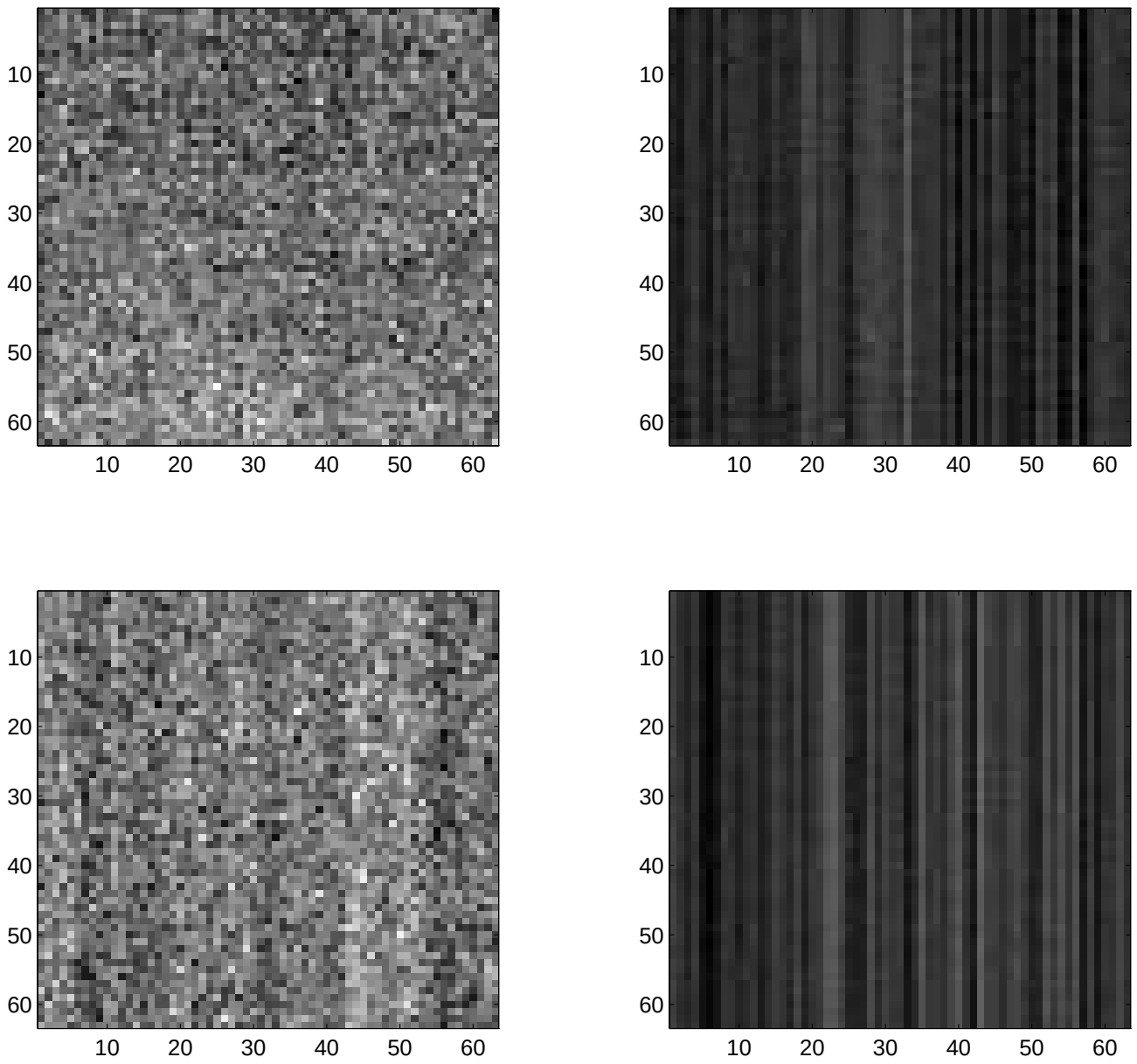

Figure 4. Top left – measured APS FPN without CDS, top right – measured APS FPN with CDS, bottom left – simulated APS FPN without CDS, and bottom right – simulated APS FPN with CDS.

4. CONCLUSIONS

We described a new FPN model for PPS and APS CMOS image sensors. The model represents FPN as the sum of two components: a pixel and a column FPN component. Each component is modeled using a first order isotropic autoregressive process, and the processes are assumed to be uncorrelated. We presented a method for estimating the parameters of the processes and reported results that justify the added model complexity compared to the simple white noise model used in CCDs. The model appears to match the measured results well, as demonstrated by the similarity between the simulated and measured FPN images.

A number of issues remain to be investigated. The estimators we used are biased and may have unacceptably large variances, which may have caused several inaccuracies in our results. More data and more analysis is needed to verify the accuracy of the estimators. It may in fact be necessary to find better estimators. The 64×64 pixel sensors we measured are too small to adequately represent FPN in real sensors. In particular for a large sensor there may be a need to model the effect of systematic device variation across the sensor. Finally, a weakness of our model is that it does not separately model gain and offset FPN components. Fowler et al.[3] report preliminary gain FPN results. However, no method for estimating gain FPN correlation was provided. To use our model for characterizing gain FPN we need to fit the model to several levels of illumination resulting in a very large amount of collected data and a large number of parameters to be estimated. A model with less parameters needs to be developed.

ACKNOWLEDGEMENTS

We wish to thank HP, Intel, and the Center for Integrated Systems (CIS) for their support of this project. In addition we wish to thank Hui Tian for performing the experiments, and Brian Wandell for his comments and suggestions.

APPENDIX A. PIXEL PARAMETER ESTIMATION

To estimate the model parameters b and σ_V^2 we consider an array with $N = M = 2l + 1$ and with zero boundary conditions and arrange equation 10 in vector notation using a raster scan pixel format to obtain

$$\mathbf{V} = \mathbf{A}\mathbf{X}, \tag{21}$$

where $\mathbf{V} = [V_{1,1}\ V_{1,2}\ \ldots V_{1,M}\ V_{2,1}\ \ldots V_{N,M}]^T$, and $\mathbf{X} = [X_{1,1}\ X_{1,2}\ \ldots X_{1,M}\ X_{2,1}\ \ldots X_{N,M}]^T$. Using this notation it can be verified that the covariance matrix of $\mathbf{X}$ is

$$\Sigma_X = \sigma_V^2 \mathbf{A}^{-1}\mathbf{A}^{-T}. \tag{22}$$

The finite image size and zero boundary conditions result in Σ_X which is not isotropic. For example, $\sigma^2_{X_{i,j}}$ is not a constant and depends on the pixel distance from the edge of the array. In our isotropic model $\sigma_{X_{i,j}}$ is a constant. The error caused by this model truncation can be minimized by choosing a large enough array size and using the values for the pixel at the center of the array. Let $\mathbf{A}^{-1}\mathbf{A}^{-T}(2l^2 + 2l + 1, 2l^2 + 2l + 1)$ be the center entry of the matrix $\mathbf{A}^{-1}\mathbf{A}^{-T}$, we estimate b by finding a value $0 \le \overline{b} \le \frac{1}{4}$ such that equation 23 is minimized.

$$\left| \frac{\overline{R_X(0,1)}}{\overline{\sigma_X^2}} - \frac{\mathbf{A}^{-1}\mathbf{A}^{-T}(2l^2 + 2l + 1, 2l^2 + 2l + 2)}{\mathbf{A}^{-1}\mathbf{A}^{-T}(2l^2 + 2l + 1, 2l^2 + 2l + 1)} \right| \tag{23}$$

We then use $\overline{b}$ to compute $\overline{\mathbf{A}}$. The estimate of σ_V^2 is then found by

$$\overline{\sigma_V^2} = \frac{\overline{\sigma_X^2}}{(\overline{\mathbf{A}})^{-1}(\overline{\mathbf{A}})^{-T}(2l^2 + 2l + 1, 2l^2 + 2l + 1)}. \tag{24}$$

For the results reported in the paper we used values for l in the range of 7 to 13.

REFERENCES

1. J. Janesick *et al.*, "Charge-coupled-device response to electron beam energies of less than 1 keV up to 20 keV," *Optical Engineering* **26**, pp. 686–91, August 1987.
2. D. Yang, B. Fowler, A. El Gamal, H. Min, M. Beiley, and K. Cham, "Test Structures for Characterization and Comparative Analysis of CMOS Image Sensors," in *Proceedings of SPIE*, (Berlin, Germany), October 1996.
3. B. Fowler, A. El Gamal, and D. Yang, "A Method for Estimating Quantum Efficiency for CMOS Image Sensors," in *Proceedings of SPIE*, (San Jose, CA), January 1998.